

3-15-2012

Temperature Dependent Droplet Impact Dynamics on Flat and Textured Surfaces

Azar Alizadeh

Vaibhav Bahadur

Sheng Zhong

Wen Shang

Ri Li

See next page for additional authors

Please take a moment to share how this work helps you [through this survey](#). Your feedback will be important as we plan further development of our repository.

Follow this and additional works at: http://ideaexchange.uakron.edu/polymer_ideas

 Part of the [Polymer Science Commons](#)

Recommended Citation

Alizadeh, Azar; Bahadur, Vaibhav; Zhong, Sheng; Shang, Wen; Li, Ri; Ruud, James; Yamada, Masako; Ge, Liehui; Dhinojwala, Ali; and Sohal, Manohar, "Temperature Dependent Droplet Impact Dynamics on Flat and Textured Surfaces" (2012). *College of Polymer Science and Polymer Engineering*. 17.

http://ideaexchange.uakron.edu/polymer_ideas/17

This Article is brought to you for free and open access by IdeaExchange@UAkron, the institutional repository of The University of Akron in Akron, Ohio, USA. It has been accepted for inclusion in College of Polymer Science and Polymer Engineering by an authorized administrator of IdeaExchange@UAkron. For more information, please contact mjon@uakron.edu, uapress@uakron.edu.

Authors

Azar Alizadeh, Vaibhav Bahadur, Sheng Zhong, Wen Shang, Ri Li, James Ruud, Masako Yamada, Liehui Ge, Ali Dhinojwala, and Manohar Sohal

Temperature dependent droplet impact dynamics on flat and textured surfaces

Azar Alizadeh,^{1,a)} Vaibhav Bahadur,¹ Sheng Zhong,¹ Wen Shang,¹ Ri Li,¹ James Ruud,¹ Masako Yamada,¹ Liehui Ge,² Ali Dhinojwala,² and Manohar Sohal³

¹General Electric Global Research, Niskayuna, New York 12309, USA

²Department of Polymer Science, The University of Akron, Ohio 44325, USA

³Idaho National Lab, Idaho Falls, Idaho 83145, USA

(Received 15 November 2011; accepted 22 January 2012; published online 15 March 2012)

Droplet impact dynamics determines the performance of surfaces used in many applications such as anti-icing, condensation, boiling, and heat transfer. We study impact dynamics of water droplets on surfaces with chemistry/texture ranging from hydrophilic to superhydrophobic and across a temperature range spanning below freezing to near boiling conditions. Droplet retraction shows very strong temperature dependence especially on hydrophilic surfaces; it is seen that lower substrate temperatures lead to lesser retraction. Physics-based analyses show that the increased viscosity associated with lower temperatures combined with an increased work of adhesion can explain the decreased retraction. The present findings serve as a starting point to guide further studies of dynamic fluid-surface interaction at various temperatures. © 2012 American Institute of Physics. [<http://dx.doi.org/10.1063/1.3692598>]

Many surface engineering applications involve impingement of water droplets; the performance of the surface depends significantly on the nature of fluid-surface interaction. Furthermore, droplet impingement can occur in a very wide temperature range. An illustration in the low temperature regime is the use of superhydrophobic surfaces for anti-icing^{1–8} applications, where the study of droplet impact dynamics is vital to estimate the interfacial contact area which provides nucleation sites for icing. At the other end of temperature spectrum, a study of impact dynamics on various surfaces has applications in the areas of spray cooling and boiling heat transfer.^{9,10} The phenomenon of condensation¹¹ in heat exchangers also involves the dynamic interaction of liquid droplets on surfaces. Understanding the influence of temperature on the fluid-surface interactions is therefore vital for controlling phase change phenomena.

Droplet impact dynamics has previously been studied for different surface-liquid-temperature combinations; however most of the studies are confined to narrow parameter ranges. Furthermore, in the field of superhydrophobicity, most existing studies have considered static droplet-fluid interactions only.^{12–15} Impact dynamics on superhydrophobic surfaces has been studied^{16–19} for multiple surface architectures (morphology and chemistry) under various impact conditions (droplet size and velocity) using both experimental and theoretical approaches; however most of these studies were at room temperature conditions. There are very few studies^{1,2,20–22} on temperature dependent droplet impact dynamics on various surfaces.

An analysis of the literature thus indicates that there is no available comprehensive study that analyzes the influence of temperature, surface chemistry, and texture over a wide parameter space. In this paper, *the temperature dependency of impact dynamics on various surfaces is studied*. Experi-

ments and analyses are presented to quantify the influence of the above parameters on the interfacial contact area at all stages during droplet spreading and retraction. The interfacial contact area is the critical parameter which determines the system performance; as an illustration, it determines the onset of freezing in icing environments and heat transfer rates in condensation applications.

Droplet impact dynamics on six surfaces (with wettability ranging from hydrophilic to superhydrophobic) were studied (Table I) in the temperature range of -15 to 85 °C. These surfaces were selected to enable a study of the influence of surface chemistry as well as texture on impact dynamics (see supplementary material³²).

Room temperature deionized water droplets (diameter 2 mm) were impacted on these surfaces, with the surface temperature varying between -15 °C and 85 °C. The tests were done at an impact velocity of 2.2 m/s, which corresponds to a Reynolds number $Re = \frac{Vd\rho}{\mu} = 4400$ and a Weber number $We = \frac{\rho V^2 d}{\gamma} = 138$ at room temperature (d is the initial droplet diameter, ρ is the density, V is the impact velocity, and γ is the surface tension of water). At higher Weber numbers, the droplet can rupture¹⁹ upon impact or pin on textured surfaces due to the Cassie-Wenzel transition.²³ All experiments were conducted in a nitrogen environment resulting in a relative humidity of less than 2%. The wetting dynamics was captured using high speed imaging of the impingement,

TABLE I. Morphological and static wettability characteristics of representative surfaces.

Sample	Morphology	Static contact angle	Roll off angle
Si	Flat	15°	No roll off
Si-PEG	Flat	44°	No roll off
Si-Trifluoro	Flat	80°	No roll off
Si-F	Flat	104°	No roll off
Si-Stex-F	Single textured	145°	37°
Si-DTex-F	Double textured	149°	11°

^{a)} Author to whom correspondence should be addressed. Electronic mail: Alizadeh@research.ge.com.

spreading, retraction, and stabilization phase of droplet impact. A high-speed Phantom V7.3 camera (from Vision Research) with video recording capabilities at 3000 frames per second was used.

One of the focal points of this work is to understand the intricacies of droplet impact dynamics on a variety of surfaces and to differentiate between static and dynamic wettability in terms of the final droplet-surface contact area. Representative high-speed images of room temperature water droplet impact on Si-PEG (hydrophilic) and Si-DTex-F (superhydrophobic) substrates at room temperature are shown in Figure 1(a). After reaching the maximum spread diameter, the droplets recoil and oscillate before reaching a final state. Wetting dynamics is quantified by measuring the droplet radius from the high speed video images (Figure 1(b)). Figure 1(b) shows the transient variation of the spread diameter, at room temperature, on five substrates. Very limited recoil is observed for the Si and Si-PEG surfaces, whereas significantly larger recoils are seen on Si-Trifluoro and Si-F surfaces. The droplets, however, remain completely pinned to these surfaces during retraction. In contrast, droplets bounce off the superhydrophobic Si-STex-F and Si-DTex-F substrates. Each droplet may experience several bounces on a superhydrophobic surface before coming to rest. It should be noted that while the impact dynamics on the two textured surfaces is rather similar under current experimental conditions, the double textured morphology is more desirable due to its higher resistance to wetting pressures. The maximum spread and the final state

spread diameters are a function of the initial droplet size, droplet velocity, and water-surface tension. However, the final state diameter is a much stronger function of the surface hydrophobicity (see supplementary material)³². The water-substrate contact area, subsequent to impact, recoil, and equilibration, can be estimated from the final state diameter. Figure 1(c) highlights the difference between the droplet-surface contact area under dynamic and static conditions. It is seen that the final contact area after droplet impact can be drastically different from the contact area of a static (or gently positioned) droplet on that surface, especially for hydrophilic surfaces. The trend in Figure 1(c) may not reflect the behavior of superhydrophilic substrates with very low contact angles ($<10^\circ$). In this case, the static contact area would be very small, thus the ratio of dynamic to static contact area should approach 1. These observations underscore the limited utility of static wettability measurements in understanding dynamic wettabilities, which as mentioned earlier are prevalent in many practical applications.

The influence of surface temperature on impact dynamics was investigated by varying the substrate temperature between -15°C and 85°C while maintaining the initial droplet temperature at 22°C . Figures 2(a)–2(c) show the transient spread diameter curves at three surface temperatures for the hydrophilic (Si-PEG), hydrophobic (Si-F) and superhydrophobic (Si-DTex-F) substrates, respectively. The effect of substrate temperature is very pronounced for the hydrophilic substrate, where a significant slowing down of

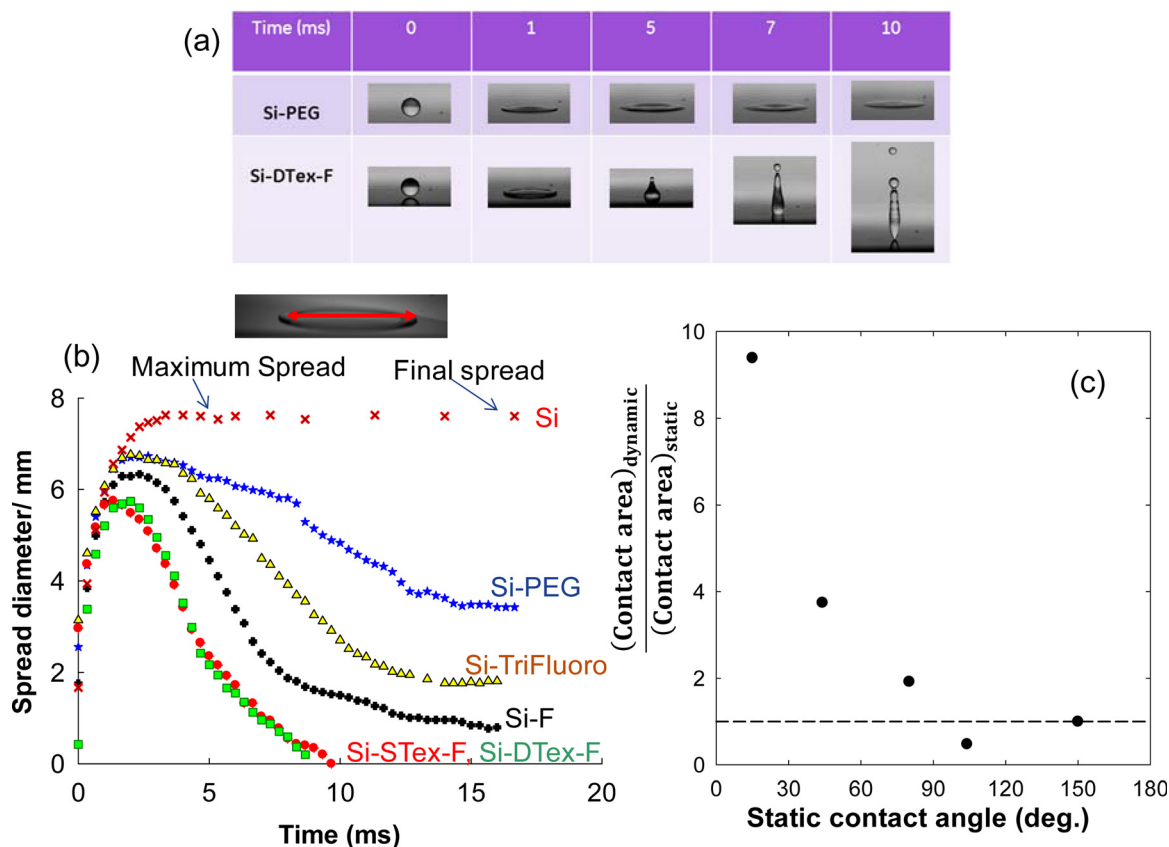


FIG. 1. (Color online) (a) High speed video images of droplet impact and wetting on hydrophilic (Si-PEG) and superhydrophobic (Si-DTex-F) substrates under room temperature conditions. (b) Transient spread diameter on Si, Si-PEG, Si-Trifluoro, Si-F, Si-STex-F, and Si-DTex-F substrates. (c) Comparison between dynamic (impact) and static contact areas. The dynamic impact area was calculated from the final state spread diameters in (b), while the static contact area was calculated from the experimentally measured contact angles assuming spherical cap geometry.

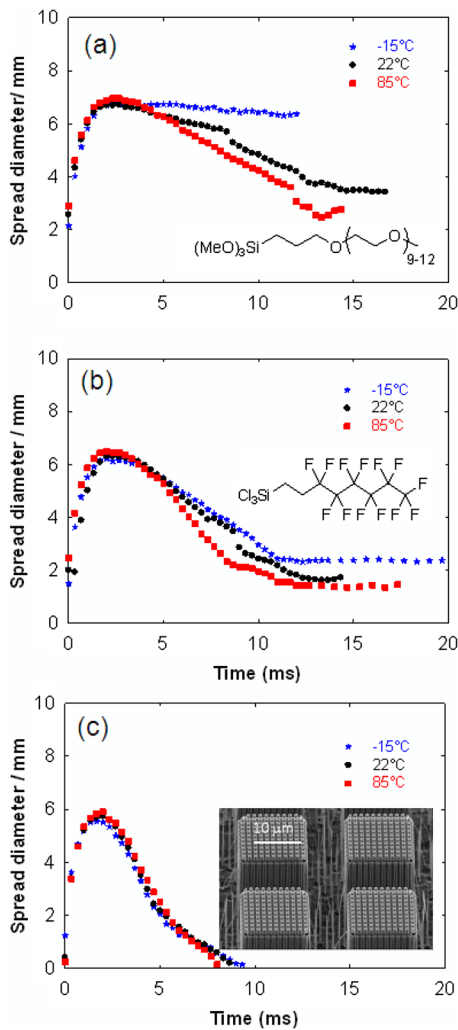


FIG. 2. (Color online) Transient spread diameter at substrate temperatures of -15°C , 22°C and 85°C on (a) Si-PEG, (b) Si-F, and (c) Si-DTex-F surfaces.

the retraction process is observed at lower temperatures. Substrate temperature has a similar but weaker effect on the hydrophobic Si-F substrate. However, the effect of temperature is completely negligible for the single and double textured superhydrophobic samples, as shown in Figure 2(c). It should be noted that the low temperature experiments are not impacted by ice nucleation at below freezing temperatures. This was verified by conducting control experiments, wherein salt water droplets were impinged on these surfaces instead of pure de-ionized (DI) water. Addition of the salt reduces the freezing point to -30°C . Very similar results were obtained on both pure DI and salt water droplets indicating that ice nucleation is not a significant consideration in the timescales of droplet spreading and retraction.³²

A simple physics-based model can explain the above observations. The initial energy of the droplet before impact consists of the kinetic and surface energy components.¹⁹ During the spreading and retraction phases, viscous dissipation and contact line friction²⁴ cause energy dissipation which reduces the energy available for recoil. This energy dissipation is significantly increased at lower temperatures, especially for hydrophilic surfaces. On such surfaces, the large contact area leads to a rapid heat transfer and cooling of the liquid layer in proximity to the surface. The increased

viscosity increases the viscous dissipation which reduces the available energy for retraction. The viscous losses can be quantified²⁵ using the following equation for flat surfaces:

$$\text{Viscous_loss} = \frac{\pi}{3} \rho V^2 d_{\max}^2 \frac{1}{\sqrt{Re}}, \quad (1)$$

where d_{\max} is the maximum spread diameter and Re is the Reynolds number corresponding to droplet impact conditions. (The other parameters in this equation were defined earlier.) The influence of viscosity on droplet impact dynamics is quantified in the Reynolds number. The viscosity of water increases²⁶ by a factor of 10 from 85°C to -15°C . At lower temperatures, the increased viscous dissipation losses reduce the energy available for retraction; thus weaker retraction is seen at lower temperatures. It is important to note that the influence of substrate temperature in the timescales of droplet impact (~ 10 ms) is felt only in a thin layer of the droplet near the wall. The thickness of this layer is about $35 \mu\text{m}$ for a thermal diffusivity of $1.3 \times 10^{-7} \text{ m}^2/\text{s}$ for water. Although the thickness of this layer is small relative to the droplet size, majority of the viscous dissipation losses (due to wall shear) occur at the substrate-water interface. The viscosity increase in this cooled thin layer is, therefore, sufficient to affect droplet retraction drastically at lower temperatures. It should be noted that other temperature dependent properties of the droplet, such as density or liquid-vapor surface tension, will not be significantly affected during this short timescale of impact. It should also be noted that contact line friction (which causes hysteresis) also leads to energy dissipation; in this study, it is assumed that the contact line friction does not change with substrate temperature.

As shown in Figure 2, the effect of surface temperature on droplet impact dynamics is not uniform across the different samples. The strong coupling between the surface temperature and surface chemistry is clearly shown when examining the droplet retention factor on the surface, which is defined as $\frac{(\text{Contact area})_{\text{final}}}{(\text{Contact area})_{\text{maximum}}}$. The maximum and final contact areas are estimated from the droplet maximum spread and final state spread diameters. Figure 3 shows the variation of the retention factor as a function of $(1 + \cos \theta) * \text{normalized viscous loss}$. For each surface, the viscous dissipation losses are normalized with respect to the corresponding viscous dissipation value for impact at 22°C . The experimentally determined retention factors fall on the same line which passes through the origin. In other words, the retraction factor can be written as

$$\text{Retention factor} = \underbrace{\alpha * (1 + \cos \theta)}_{\text{Adhesion}} * \underbrace{\frac{\text{Viscous}_{\text{loss}}(T)}{\text{Viscous}_{\text{loss}}(T_0)}}_{\text{Viscous dissipation}}. \quad (2)$$

The first term in Eq. (2) is related to energy losses due to adhesion (the work of adhesion is $W_a = \gamma(1 + \cos \theta)$), while the second term represents the energy losses associated with viscous dissipation, as described earlier. Accordingly, high viscous dissipation losses (lower temperatures) combined with strong water-surface interactions (large adhesion) lead to very low mobility of water during recoil, where a retention

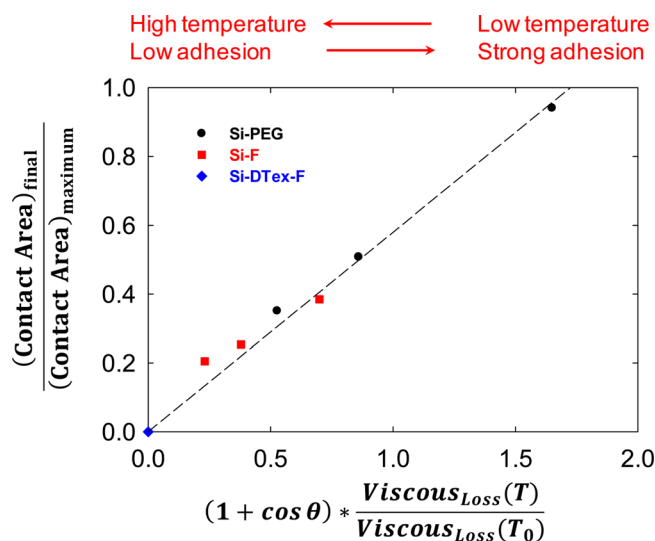


FIG. 3. (Color online) Linear variation of retention factor (defined as the ratio of final and maximum contact areas) with $(1 + \cos \theta) \times$ (normalized viscous loss), where θ represents the static contact angle.

factor of almost 1 is observed for highly hydrophilic surfaces. In contrast, complete retraction of water is observed on superhydrophobic surfaces, which are represented with the blue symbol at the origin in Figure 3. This observation, which implies low viscous dissipation and low adhesion losses, is in full agreement with previously observed low drag properties of superhydrophobic surfaces.²⁷ The temperature invariant nature of droplet impact on textured superhydrophobic surfaces can be explained by heat transfer considerations. The magnitude of heat transfer from a superhydrophobic surface to a droplet is significantly reduced due to the presence of a thermal resistance (air gap) beneath the droplet,²⁸ which limits the increase in viscosity due to droplet cooling. Finally, the slope of the line in Figure 3 (the dimensionless parameter α in Eq. (2)) is equal to 0.3 for the current experimental data. The magnitude of this slope depends on the physical properties (such as density and vapor-liquid surface tension) of the droplet. Therefore, one may anticipate this parameter to vary for a different combination of initial droplet and substrate temperatures.

The first-order analyses developed here provide a direct qualitative match with the experimental findings; the development of more detailed models for predicting impact dynamics is beyond the scope of the present work. It should be noted that existing analytical^{29,30} or numerical³¹ models for impact dynamics, in their current formulations, cannot fully capture the detailed aspects of the work presented here. Existing models have been developed for use in limited contact angle ranges and are not setup to directly include the coupling of surface temperature and chemistry.

In conclusion, this work presents the strong influence of temperature on droplet impact dynamics on various surfaces. The strong temperature dependence on hydrophilic surfaces indicates that more analysis is needed before using such surfaces in applications such as wicking or oil-water separation. Similarly, the role of viscous dissipation and friction is particularly important at subzero temperatures and should be

investigated in more detail. In contrast, textured superhydrophobic surfaces show temperature invariant impact dynamics; this significantly increases their desirability for applications in both low and high temperature regimes.

The authors are very thankful to Margaret Blohm, Chris Keimel, Oliver Boomhower, Ken Conway, and Scott Miller for their assistance of this work and helpful discussions. The Nanotechnology Advanced Technology Program at GE Global Research, the Department of Energy (Award No. DE-AC07-05ID14517) and National Science foundation (Grant No. 1006764) are acknowledged for financial support (this manuscript has been authored by Battelle Energy Alliance, LLC under Contract No. DE-AC07-05ID14517 with the US Department of Energy. The publisher, by accepting the article for publication, acknowledges that the United States Government retains a nonexclusive, paid-up, irrevocable, world-wide license to publish or reproduce the published form of this manuscript or allow others to do so, for United States Government purposes).

- ¹L. Mishchenko, B. Hatton, V. Bahadur, J. A. Taylor, T. Krupenkin, and J. Aizenberg, *ACS Nano* **4**, 7699 (2010).
- ²V. Bahadur, L. Mishchenko, B. Hatton, J. A. Taylor, J. Aizenberg, and T. Krupenkin, *Langmuir* **27**, 14143 (2011).
- ³A. J. Meuler, G. H. McKinley, and R. E. Cohen, *ACS Nano* **4**, 7048 (2010).
- ⁴L. Cao, A. K. Jones, V. K. Sikka, J. Wu, and D. Gao, *Langmuir* **25**, 12444 (2009).
- ⁵P. Tourkine, M. Le Merrer, and D. Quéré, *Langmuir* **25**, 7214 (2009).
- ⁶S. Jung S, M. Dorrestijn, D. Raps, A. Das, C. M. Megaridis, and D. Poulikakos, *Langmuir* **27**, 3059 (2011).
- ⁷S. A. Kulinich, S. Farhadi, K. Nose, and X. W. Du, *Langmuir* **27**, 25 (2011).
- ⁸K. K. Varanasi, T. Deng, J. D. Smith, M. Hsu, and N. Bhate, *Appl. Phys. Lett.* **97**, 234102 (2010).
- ⁹A. Bianche, C. Clanet, and D. Quéré, *Phys. Fluids* **15**, 1632 (2003).
- ¹⁰N. Z. Mehdizadeh and S. Chandra, *Proc. R. Soc. A* **462**, 3115 (2006).
- ¹¹I. C. Bang and J. H. Jeong, *Nucl. Eng. Technol.* **43**, 217 (2011).
- ¹²D. Quéré, *Annu. Rev. Mater. Res.* **38**, 71 (2008).
- ¹³L. Cao and T. J. McCarthy, *Langmuir* **25**, 14105 (2009).
- ¹⁴M. Nosonovsky and B. Bhushan, *J. Phys. Condens. Matter* **20**, 225009 (2008).
- ¹⁵A. L. Yarin, *Annu. Rev. Fluid Mech.* **38**, 159 (2006).
- ¹⁶Y. C. Jung and B. Bhushan, *Langmuir* **24**, 6262 (2008).
- ¹⁷M. Reyssat, A. Pépin, F. Marty, Y. Chen, and D. Quéré, *Europhys. Lett.* **74**, 306 (2006).
- ¹⁸D. C. Vadiello, A. Soucemarianadin, C. Dellatre, and D. C. D. Roux, *Phys. Fluids* **21**, 122002 (2009).
- ¹⁹B. Wang, Y. Zhao, and T. Yu, *J. Adhes. Sci. Technol.* **25**, 93 (2011).
- ²⁰X. Li, X. Ma, and Z. Lan, *AIChE J.* **55**, 1983 (2009).
- ²¹R. Karmouch and G. G. Ross, *J. Phys. Chem. C* **114**, 4063 (2010).
- ²²M. Pasandideh-Fard, S. D. Aziz, S. Chandra, and J. Mostaghimi, *Int. J. Heat Fluid Flow* **22**, 201 (2001).
- ²³V. Bahadur and S. V. Garimella, *Langmuir* **25**, 4815 (2009).
- ²⁴H. Ren, R. B. Fair, M. G. Pollack, and E. J. Shaughnessy, *Sens. Actuators B* **87**, 201 (2002).
- ²⁵M. Pasandideh-Fard, Y. M. Qiao, S. Chandra, and J. Mostaghimi, *Phys. Fluids* **8**, 650 (1996).
- ²⁶J. Hallett, *Proc. Phys. Soc.* **82**, 1046 (1963).
- ²⁷L. Mahadevan and Y. Pomeau, *Phys. Fluids* **11**, 2449 (1999).
- ²⁸P. Tourkine, M. L. Merrer, and D. Quere, *Langmuir* **25**, 7214 (2009).
- ²⁹I. V. Roisman, R. Rioboo, and C. Tropea, *Proc. R. Soc. A* **458**, 1411 (2002).
- ³⁰H. Y. Kim and J. H. Chun, *Phys. Fluids* **13**, 643 (2001).
- ³¹K. Yokoi, D. Vadiello, J. Hinch, and I. Hutchings, *Phys. Fluids* **21**, 072102 (2009).
- ³²See supplementary material at <http://dx.doi.org/10.1063/1.3692598> for further details of the fabrication and measurement of static wettability on these surfaces.